Tectonics

Supporting Information for

Megathrust Heterogeneity, Crustal Accretion, and a Topographic Embayment in Western Nepal Himalaya: Insights from the Inversion of Thermochronological Data

Suoya Fan[1]; Michael A. Murphy[1]; David M. Whipp[2]; Joel E. Saylor[3]; Pete Copeland[1]; Andrew K. Hoxey[4]; Michael H. Taylor[4]; Daniel F. Stockli[5]

[1]Department of Earth and Atmospheric Sciences, University of Houston, Houston, Texas 77204, USA

[2]Institute of Seismology, Department of Geosciences and Geography, University of Helsinki, Helsinki, Finland

[3]Department of Earth, Ocean and Atmospheric Sciences, University of British Columbia, Vancouver, British Columbia, Canada

[4]Department of Geology, University of Kansas, Lawrence, Kansas 66045, USA

[5]Department of Geological Sciences, Jackson School of Geosciences, University of Texas at Austin, Austin, Texas 78712, USA

Contents of this file

Introduction

The supporting informations include (Table S1) a table that shows the information of the analyzed samples in this study, (Text S1) a description of the analytical procedure used for the acquisition of zircon (U-Th)/He thermochronological data, and (Figure S1) a map of the cooling ages used in the inversion models in this study, and (Text S2) is a reference list of this supporting information. The references in Text S2 are also included in the main paper.

Sample	Longitude (°E)	Latitude (°N)	Elevation (m)	Lithology	Unit
Dolpo-4	83.149367	29.5641	4741	muscovite schist	STD Shear Zone
DF-3	83.87095	29.11715	4275	leucogranite	GHS
DF-4	83.879633	29.13475	4159	leucogranite	GHS
DH-10	82.822972	29.0405	2546	garnet-muscovite-biotite schist	MCT Shear Zone
DG10	83.157167	28.653	3855	kyanite-garnet-biotite gneiss	GHS
DG12	83.2305	28.588833	2577	graphitic schist	MCT Shear Zone
DG22	82.992833	28.760833	4225	kyanite-garnet-biotite gneiss	MCT Shear Zone
DG29	82.943	28.859833	3703	quartzite	LHS
DG30	82.911167	28.932833	2932	quartzite	LHS
DG38	82.832667	28.992167	2249	quartzite	LHS
TB10-9	82.50502	29.72841	3620	leucogranite	GHS
TB10-12	82.45309	29.58116	3408	leucogranite	GHS

Table S1. The number, location, lithology, and unit of each sample analyzed in this study.

Text S1.

Analytical procedure of zircon (U-Th)/He dating:

Zircon (U-Th)/He thermochronology was performed using standard laboratory procedures at the University of Texas UTChron Laboratory (Wolfe and Stockli, 2010). Individual zircon mineral grains were screened for quality, size, shape, and inclusions. Individual single-grain aliquots were measured for standard morphometric α-ejection age (Ft) corrections. Zircon aliquots were wrapped in Pt foil tubes, laser heated for 10 minutes at ~1300 °C and subsequently reheated until completely degassed (<1% He re-extract). The released ^{4}He was spiked with ^{3}He tracer, cryogenically purified/concentrated, and analyzed with a Blazers Prisma QMS-200 quadrupole mass spectrometer. After complete degassing, zircon aliquots were unwrapped from Pt foil, spiked (U, Th, and Sm) and dissolved for U, Th, and Sm determination using standard U-Pb double pressure-vessel digestion procedures (HF- HNO_3 and HCl). Spiked aliquot solutions were analyzed for U, Th, and Sm using the Thermo Element2 HR-ICP-MS. Raw ages were calculated from ^{4}He, U, Th, and Sm concentrations, and corrected ages were calculated using standard α-ejection correction. Reported age uncertainties (~8%, 2σ) reflect the reproducibility of replicate analyses of standard samples.
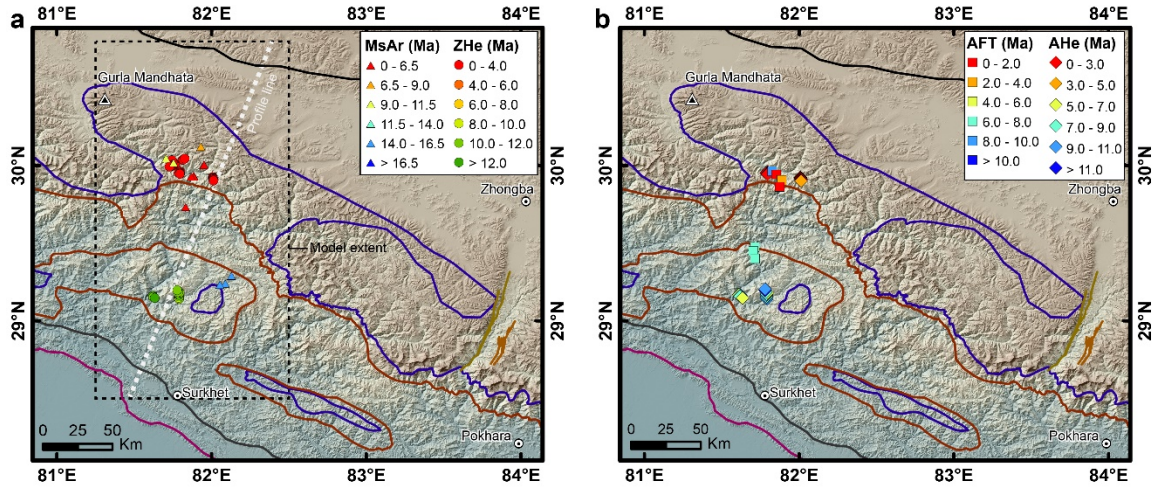
Figure S1. Distribution of the cooling ages that are used in the inversion models. (a) shows the cooling ages of muscovite $^{40}Ar/^{39}Ar$ ages (MSAr) and zircon (U-Th)/He ages (ZHe); (b) shows the apatite fission track ages (AFT) and apatite (U-Th)/He ages (AHe). The dash box in (a) shows the extent of the themrokienmatic models in this study. The data is from previously published studies (McCallister et al., 2014; Mercier, 2014; Harvey, 2015; Nagy et al., 2015; van der Beek et al., 2016; Soucy La Roche et al., 2018; Braden et al., 2020).

Text S2.

The references that cited in this supporting information:

Braden, Z., Godin, L., Kellett, D. A., and Yakymchuk, C., 2020, Spatio-temporal challenges in dating orogen-scale shear zones: The case of the Himalayan Main Central thrust: Tectonophysics, v. 774, p. 228246, https://doi.org/10.1016/j.tecto.2019.228246.

Harvey, J. E., 2015, Along-strike tectonic variability in the central Himalaya, University of California, Santa Barbara.

McCallister, A. T., Taylor, M. H., Murphy, M. A., Styron, R. H., and Stockli, D. F., 2014, Thermochronologic constraints on the late Cenozoic exhumation history of the Gurla Mandhata metamorphic core complex, Southwestern Tibet: Tectonics, v. 33, no. 2, p. 27-52, https://doi.org/10.1002/2013tc003302.

Mercier, J., 2014, Structure and evolution of orogenic wedges : a multidisciplinary study on the Himalayan case]: Université de Grenoble.

Nagy, C., Godin, L., Antolín, B., Cottle, J., and Archibald, D., 2015, Mid-Miocene initiation of orogen-parallel extension, NW Nepal Himalaya: Lithosphere, v. 7, no. 5, p. 483-502, https://doi.org/10.1130/l425.1.

Soucy La Roche, R., Godin, L., Cottle, J. M., and Kellett, D. A., 2018, Preservation of the Early Evolution of the Himalayan Middle Crust in Foreland Klippen: Insights from the Karnali Klippe, West Nepal: Tectonics, v. 0, no. 0, https://doi.org/10.1002/2017tc004847.

van der Beek, P., Litty, C., Baudin, M., Mercier, J., Robert, X., and Hardwick, E., 2016, Contrasting tectonically driven exhumation and incision patterns, western versus central Nepal Himalaya: Geology, v. 44, no. 4, p. 327-330, https://doi.org/10.1130/g37579.1.